IEEE Access
Multidisciplinary | Rapid Review | Open Access Journal

Received February 19, 2019, accepted March 8, 2019, date of publication March 20, 2019, date of current version April 5, 2019.

Digital Object Identifier 10.1109/ACCESS.2019.2906122

Resistor-Capacitor Combined DC Bias Protection of AC Power Grid of Jiuquan-Hunan ±800 kV Transmission Lines

JIANGONG ZHANG[1,2], BOCHENG LI[2], BO TANG[2], JIAWEI YANG[2], AND LI HUANG[2]
[1]State Key Laboratory of Power Grid Environmental Protection, Wuhan Branch of China Electric Power Research Institute, Wuhan 430074, China
[2]College of Electrical Engineering and New Energy, China Three Gorges University, Yichang 443002, China

Corresponding authors: Bocheng Li (aslunar@vip.qq.com) and Bo Tang (tangboemail@sina.com)

This work was supported in part by the State Key Laboratory of Power Grid Environmental Protection under Grant GYW51201700590, and in part by the Science and Technology Program of State Grid Corporation of China (SGCC) under Grant GY71-16-011.

ABSTRACT DC bias was observed in transformers of the ac system surrounding Jiuquan–Hunan ±800 ultra-high voltage direct current (UHVDC) transmission lines in China, which were operating in the simulation of the unipolar-earth ground mode. Applying conventional dc bias protection methods in this case that showed certain disadvantages including large time and calculation resource demand, this paper proposed to use an *RC* combined method to control the dc bias in this ac system. By determining appropriate capacities of resistor and capacitor based on the requirement of insulation and zero sequence current, it is able to stabilize a system under a single-phase ground fault with a dc suppression device installed in the neutral point. In addition, after analyzing the regularity of the dc distribution in the ac system with different substation connections, we also proposed an implementation strategy of dc suppression in power grid. The protection method was further tested in a numerical dc power grid model and verified by field experiments. The result showed that in the most serious case of the model system, when a current of 5000 A flows into the ground, the dc level of the neutral point of substation under protection by the proposed method is well controlled. This indicates that the proposed method is applicable to the dc bias protection of the dc–ac system operating at the highest voltage ever worked.

INDEX TERMS DC bias, RC combined method, UHVDC transmission lines, unipolar-earth ground operation.

I. INTRODUCTION

DC bias describes the phenomenon caused by direct current flows into transformers [1], [2]. In Mar. 2017, when Jiuquan-Hunan ±800 kV UHVDC (Ultra-High Voltage Direct Current) transmission lines (JH800) in China was simulating operation under unipolar-earth ground mode with non-full power, serious DC bias was induced in transformers of nearby AC systems connected to the UHVDC lines [3], [4]. Therefore, to enable the UHVDC system to operate with full power while ensuring the security of the whole power grid, a suitable DC protection strategy is essential.

Recent research of DC bias protection mainly focused on two aspects, namely 1) suppression methods of DC bias and 2) implementation strategies of DC suppression in power grid [5]–[11]. For, DC bias suppression methods, resistor method (RM), capacitor method (CM) and current injection method (CJM) are the common types to restrain the direct current in neutral points of transformers [12], while new design of transformer using two-phase magnetic material was also developed to reduce bias levels [13]–[15]. Among the methods, CJM has not been widely applied in practice due to the relative lack of economy and reliability, and the development of new transformers is still in the experimental stage. While RM and CM have been applied in most occasions, how to determine the capacity of resistors or capacitors used in these methods has not been well studied. Instead, the value is usually determined based on engineering experience, which may bring instability into the power system under DC bias protection [16].

As for the implementation strategy of DC suppression, artificial intelligence algorithms such as 'genetic algorithm' and 'particle swarm algorithm' [17]–[19], are introduced to deal with the optimization of RM or CM used in the power grid. Nevertheless, as a result of the rather complex structure of

The associate editor coordinating the review of this manuscript and approving it for publication was Snehal Gawande.

power grids, applying these algorithms will cost a lot of time and computing resources, so normally the integral grid cannot be fully analyzed [20]–[22]. Though some researchers have proposed a step-by-step strategy that determined by DC severity in neutral point, it causes an increase in the current of the partial grids.

Therefore, we proposed a RC combined method to protect the nearby transformers of JH800 from DC bias, along with the method to determine the parameters of resistor and capacitor used in the protection. Moreover, to apply this RC combined method reasonably to the power grids, we also put forward a new strategy based on DC current distribution. Further simulations were carried out to verify the proposed methods, and the results showed that target DC bias levels could be well controlled.

II. OVERALL IDEAS OF DC BIAS PROTECTION

A. DETERMINING THE PROTECTION METHOD

DC bias is caused by the direct current flows into the neutral point of transformer, so the key to solve this problem is to restrain the DC current. To achieve this goal, RM is to install a resistor device in the neutral point to reduce the amplitude of current in the whole loop of the system, while the CM has to install a capacitor, which is expected to block DC currents. However, the use of RM or CM alone may cause an abnormal increase in short circuit overvoltage and partial the direct current in partial grids

Since RM and CM has their own advantages, we wondered if it is able to combine the two, and then proposed a RC combined method, along with the device capacity determination method and implementation strategy to make the RC method work.

B. DETERMINING PERMISSION DC IN NEURAL POINT

Till now, there is no widely-accepted regulation of permission current for transformers. Thus, we proposed the permission current in Jiuquan power grid according to both transformer design parameters and existing protection experience, namely 12 A and 8 A for neutral points of 750 kV and 330 kV transformers respectively. Actually, these 750 kV and 330 kV transformer systems are made of autotransformers, which means we cannot suppress the DC from the windings inside autotransformers by using CM.

Fig. 1 shows the connection diagram of an autotransformer. When the capacitor device works, I_g is 0, so the current detected at d1, the neutral point, is 0, too. However, I_c still exists and will flow through n_1 to another transformer's windings like n_2 and form a loop, which will then induce DC bias at n_2 position that we cannot discover. Therefore, based on Kirchhoff and Magnetic flux-conservation law, we proposed to use I_{eff} as the 'equivalent bias current' to express the current in n_1 when the capacitor works in different conditions.

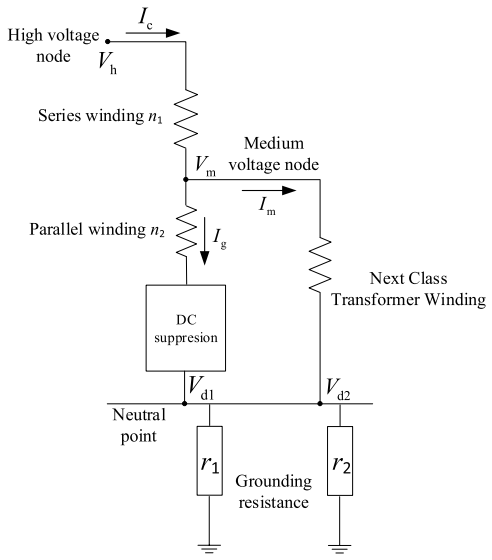

FIGURE 1. The direction of DC current inside the autotransformer.

When the capacitor is in short circuit, DC in n_1 can be expressed as

$$I_{eff} = I_{\text{m}} + I_{\text{g}} = V_{\text{m}}\,(y_{\text{md1}} + y_{\text{md2}}) - (V_{\text{d1}}\,y_{\text{md1}} + V_{\text{d2}}\,y_{\text{md2}}) \tag{1}$$

where y_{md1} and y_{md2} are the admittance parameters at each node.

When the capacitor functions, there will be

$$I_{\text{eff}} \times (n_1 + n_2) = I_c \times n_1 + I_{\text{g}} \times n_2 \tag{2}$$

In field measurement, the number of winding turns is difficult to obtain, so it can be expressed as the rated voltage ratio of the transformer

$$\frac{U_{1\text{N}}}{U_{2\text{N}}} = \frac{n_1 + n_2}{n_2} = k \tag{3}$$

So the formula is got

$$I_{\text{eff}} = \frac{1}{k} I_c + I_{\text{m}} \left(1 - \frac{1}{k}\right) = \frac{y_{\text{hm}}\,(V_{\text{h}} - V_{\text{m}})}{k} + (V_{\text{m}} - V_{\text{d2}})\,y_{md2} \left(1 - \frac{1}{k}\right) \tag{4}$$

where k is the rated voltage ratio. I_{eff} shall not exceed 4A to make the autotransformer operate normally.

III. SOLUTION OF THE KEY PROBLEMS IN RC COMBINED PROTECTION METHOD

A. NCIPLE CRITERIA FOR PARAMETER VERIFICATION

Installing a resistor or capacitor to the neutral point will change the zero-sequence impedance, which may lead to an increase in zero sequence overvoltage and current, or even cause insulation breakdown and relay protection malfunction.

Fig. 2 shows the schematic diagram of 330 kV system model with straightening device. Because 330 kV line is

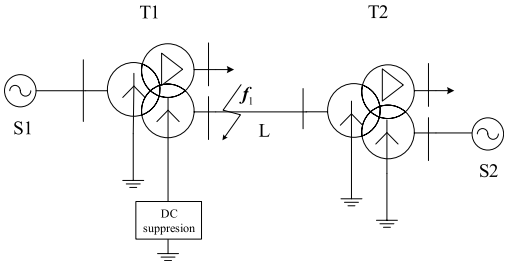

FIGURE 2. The connection of transformer system.

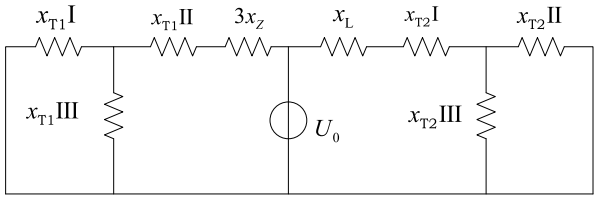

FIGURE 3. Parametric tuning model sketch.

connected to the main network, the other electrical parts of T1 and T2 connected to the two power stations can be replaced with equivalent infinite power supply S1 and S2, where L is the transmission line.

When a single-phase grounding fault occurs in f_1, the zero-sequence network of the system is shown in Fig. 3.

In this case, the zero-sequence impedance of the system is expressed as

$$Z_{0\sum} = \frac{\left(\frac{x_{T1}I \cdot x_{T1}\text{III}}{x_{T1}I + x_{T1}\text{III}} + x_{T1}II \pm 3x_Z\right)\left(\frac{x_{T2}II \cdot x_{T2}\text{III}}{x_{T2}II + x_{T2}\text{III}} + x_L\text{II} + x_{T2}I\right)}{\left(\frac{x_{T1}I \cdot x_{T1}\text{III}}{x_{T1}I + x_{T1}\text{III}} + x_{T1}\text{II} \pm 3x_Z\right) + \left(\frac{x_{T2}\text{II} \cdot x_{T2}\text{III}}{x_{T2}\text{II} + x_{T2}\text{III}} + x_L\text{II} + x_{T2}I\right)} \tag{5}$$

where, x_{T1} and x_{T2} are transformer impedance, x_L is the transmission line's impedance, $3x_Z$ is the impedance of straightening device.

The neutral overvoltage of the system is expressed as

$$U_N = \frac{3x_Z U_0}{\left(\frac{x_{T1}I \cdot x_{T1}\text{III}}{x_{T1}I + x_{T1}\text{III}} + x_{T1}\text{II} \pm 3x_Z\right)} = \frac{3x_Z E_{\sum} Z_{0\sum}}{\left(\frac{x_{T1}I \cdot x_{T1}\text{III}}{x_{T1}I + x_{T1}\text{III}} + x_{T1}\text{II} \pm 3x_Z\right)\left(Z_{0\sum} + Z_{1\sum} + Z_{2\sum}\right)} \tag{6}$$

where, $E_{\sum}$ is the voltage at f_1 before the short circuit occurs, $Z_{0\sum}$ is zero sequence impedance, $Z_{1\sum}$ is positive sequence impedance, $Z_{2\sum}$ is negative sequence impedance, U_0 is the zero sequence voltage of the short circuit point.

The zero-sequence fault current flowing through the DC suppression device is expressed as

$$I_Z = \frac{3E_{\sum} Z_{0\sum}}{\left(\frac{x_{T1}I \cdot x_{T1}\text{III}}{x_{T1}I + x_{T1}\text{III}} + x_{T1}\text{II} \pm 3x_Z\right)\left(Z_{0\sum} + Z_{1\sum} + Z_{2\sum}\right)} \tag{7}$$

According to the system requirements, U_N should be within 85 kV, and the fluctuation of I_Z amplitude should not exceed 10%.

According to equation 4-6, when a single-phase grounding short circuit occurs in the busbar f_1 of transformer T1 high voltage side, a restraining device is installed at transformer neutral point to change the zero sequence parameter of the system, but has no effect on the positive and negative sequence parameters of the system. The influence of resistance and capacitance devices on the system are acceptable. However, in order to ensure safety and reliability, the impedance value is as small as possible while satisfying the DC protection standard.

B. DETERMINING THE CAPACITIES OF RESISTOR AND CAPACITOR

Based on the setting of Fig. 2, the 330 kV system model is built in Simulink. We suppose that the L is a 30 km transmission line of ACSR. Assuming that the neutral point potential difference between T1 and T2 is 200 V, and the single-phase fault starts at 0.1 s and lasts for 0.3 s, the zero-sequence current and neutral point overvoltage under the combined action of DC bias and short-circuit fault are simulated and analyzed. When the neutral point is not connected with the resistance, the zero-sequence current of the neutral point is shown in Fig. 4.

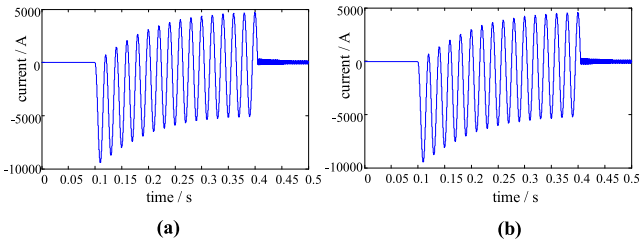

FIGURE 4. Zero sequence current with no resistor or capacitor. (a) No DC bias. (b) Be in DC bias.

When the neutral line has no bias current, the zero-sequence current waveform is shown in Fig. 4(a). From the figure, the transient current peak value is −9.449 kA, the steady-state current positive peak value is 4.899 kA, and the negative peak value is −4.801 kA. The positive and negative peaks are basically equal, indicating that the positive half wave is symmetric with the negative half wave when no bias current flows in the core, and the transformer is in normal working state. When the unequal DC voltage is added to both ends of the line, the zero-sequence current waveform is as shown in Fig. 4(b). From the figure, the transient current peak value is −9.778 kA, and the steady-state positive and negative peaks are 4.733 kA and −5.064 kA. This is due to the occurrence of DC bias current inside the core, resulting in positive and negative half-wave asymmetry. From the simulation results, it can be estimated that the DC current at this time is about 300 A, so it is necessary to install a suppressing device.

In the study of DC bias protection, a resistor of approximately 10 Ω is typically selected to configure the protection device. But 10 Ω is it's not an accurate value, and it is obviously not in line with the requirements of DC protection reliability. In order to determine an accurate value, further research is needed. The study found that the smaller the capacitive reactance value, the smaller the impact on the system, but the larger the volume, the higher the cost. It is considered that the capacitance of the capacitor is inversely proportional to the size of the capacitor and the current manufacturing level, and the capacitance of the capacitor used in the high voltage system is between 0.05 Ω and 1.0 Ω. So adding a resistor (R = 1, 2, 3, 5, 7, 10, 15 Ω) or a capacitor (C = 0.05, 0.1, 0.2, 0.4, 0.6, 0.8, 1.0 Ω) in power frequency impedance, the change of I_Z and U_N in neutral points is observed and used to determine the capacity of protection devices. Part of the results are shown in Table 1.

TABLE 1. The fault current and voltage under different resistors(part).

R (Ω)	Steady (kA)	Transient(kA)	C(Ω)	Steady(kA)	Transient(kA)
1	-9.267	4.687 -4.819	0.05	-9.446	4.980 -4.980
3	-8.829	4.621 -4.666	0.1	-9.429	4.963 -4.963
5	-8.441	4.629 -4.648	0.2	-9.408	4.946 -4.946
10	-7.576	4.548 -4.553	0.6	-9.325	4.913 -4.915
15	-6.853	4.519 -4.521	1.0	-9.243	4.901 -4.899

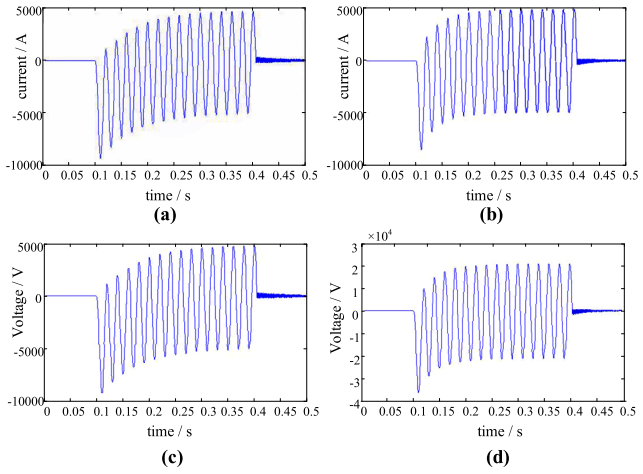

FIGURE 5. The zero sequence current and overvoltage. (a) Zero sequence current (1Ω). (b) Zero sequence current (5Ω). (c) Overvoltage (1Ω). (d) Overvoltage (5Ω).

Fig. 5 shows the zero-sequence current and over-voltage changes at the center point when 1 Ω and 5 Ω resistors are added.

Comparing Fig. 5(a) with Fig. 4(b), we can see that the positive and negative half-wave peaks of the zero-sequence current have changed when adding a 1 Ω resistor. The steady-state positive peak is reduced from 4.733 kA to 4.687 kA, and the negative peak value is −4.819 kA. The absolute difference between the two is 132 A. At this point, the positive and negative half waves gradually become the same, and the bias current is reduced by nearly 60%, which indicates that adding a 1 Ω resistor has a significant straightening effect, and the bias current can be reduced by more than a half.

However, it is worth noting that the system is connected to an external resistor, which changes the zero-sequence network parameters. This change will result in a decrease in the zero-sequence current peak. As can be seen from the figure, the transient peak value changed from −9.778 kA to −9.267 kA, a decrease of 5.2%. The steady-state peak is relatively small, with positive and negative peaks decreasing by 0.9% and 4.8%. Similarly, the variation of Fig. 5(b) can be obtained. DC suppression is better when a 5 Ω resistor is connected. The positive and negative half waves are basically the same in steady state, the difference between the absolute values of the current peaks is only 6A, and the internal bias current of the core is reduced by more than 90% to an acceptable range. But at the same time, the zero-sequence current transient peak also dropped to −8.441 kA, a decrease of 13.6%, which further deepened the impact on system protection.

After the resistor is installed, not only the influence of the line current, but the neutral point overvoltage will increase. It can be seen from the Fig. 5(b) and Fig. 5(d) when the resistance increases, the peak value of the neutral point overvoltage increases significantly. And when a 5 Ω resistor is added, the transient peak reaches −42.14 kV. According to the simulation results of Table 1, it can be obtained that with the increase of the access resistance value, the steady-state positive and negative peaks of the current tend to be consistent. When the resistance is 3 Ω, a good straightening effect is achieved. When the resistance is increased to more than 5 Ω, the change of the bias current is not obvious, and the straightening effect reaches the saturated state. At the same time, as the resistance increases, the zero-sequence current peak decreases and the overvoltage peak increases. When the 15 Ω is connected, the zero-sequence current transient peak is reduced by 29.9%, and the steady-state peak is reduced by 10.7%. At this point, the neutral point overvoltage reaches 100.1 kV. According to the Chinese Standard Value of 85kV, the system insulation may be damaged. Therefore, after comprehensively integrating all aspects, a resistor of 2 Ω to 3 Ω should be chosen.

Capacitor is characterized of blocking DC, so we only need to consider if the overvoltage and zero-sequence current satisfy the system limits. Considering that the capacitor and the resistor work differently, the capacitor needs to be charged and discharged at both ends, thus increasing the simulation duration. In the simulation, the single-phase short-circuit fault is extended to 1.4 seconds, the simulation time is 1.6 seconds, and the remaining parameters are unchanged. Fig. 6 shows the neutral zero-sequence current and overvoltage variation when a power frequency impedance of 0.05 Ω and 1.0 Ω capacitors is added. Part of the results are shown in Table 1.

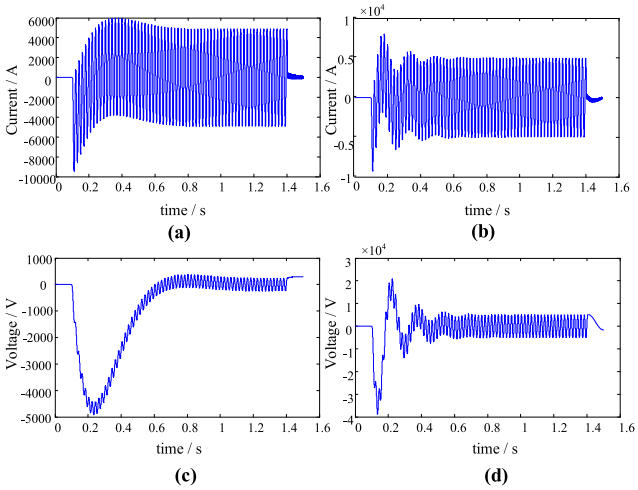

FIGURE 6. The zero-sequence current and overvoltage. (a) Zero sequence current (0.05Ω). (b) Zero sequence current (1Ω). (c) Overvoltage (0.05Ω). (d) Overvoltage (1Ω).

As shown in Fig. 6, as the impedance of the capacitor increases, the positive and negative peaks of the current are substantially equal. When connected to a 0.05 Ω impedance capacitor, the system's steady-state positive and negative peak currents are 4.980 kA and −4.980 kA. Simultaneously, when connected to a 1 Ω impedance capacitor, the value are 4.901 kV and −4.899 kA. This indicates that the size of the capacitor is independent of the bias current suppression effect and only affects the zero-sequence current amplitude.

Moreover, comparison between Fig. 6(c) and Fig. 6(d) shows that before reaching a steady state, the fluctuation of overvoltage is in positive correlation with the capacity of capacitor. This means that larger capacity can result in smaller amplitude fluctuations, i.e. less influence to system. When the capacitor of 1 Ω is connected, the maximum value of the current 5.567 kA, which is 200 A lower than the effective value of the zero-sequence current without the capacitor. And this is reduced by 3.5%, within the reliability range of the system protection action. The peak value of the voltage is 33.72 kV, which also has a large margin from the standard value of 85 kV. Combined with Table 1, after comprehensive analysis, it can be considered that any size capacitor between 0.05 Ω and 1.0 Ω meets the protection requirements. However, taking economy into consideration, 0.5 Ω capacitor could be a better choice in practice, since it also has change of current and voltage meeting the limits, while costs less.

In summary, a 2 to 3 Ω resistor and a 0.5 Ω capacitor should be selected as the protection configuration.

C. DETERMINING IMPLEMENTATION STRATEGY OF DC SUPPRESSION IN POWER GRID

The distribution of DC in transformers' system can be simply described as shown Fig. 7, where the current I mainly depends on both the topology of system and the electric potential at the ground points.

Supposed there are n substations and b branches in this transformers system, so the vector quantity of electric

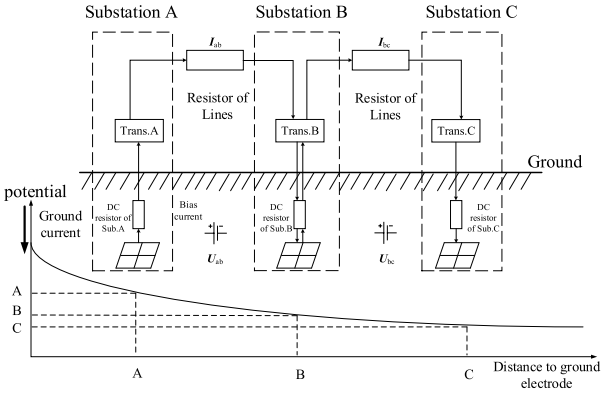

FIGURE 7. Relationship between the potential and distance.

potential and current in neural points could be expressed as

$$\mathbf{U}_\mathrm{b} = \mathbf{B}\mathbf{U}_\mathrm{n} \tag{8}$$

$$\mathbf{I}_\mathrm{n} = -\mathbf{B}^T\mathbf{I}_\mathrm{b} \tag{9}$$

where $\boldsymbol{U}_\mathrm{b}$ and $\boldsymbol{I}_\mathrm{b}$ are the vector quantity of branch currents and voltages, $\boldsymbol{B}$ is a $(b \times n)$ square.

For branches

$$\mathbf{I}_b = \mathbf{G}_\mathrm{b}\mathbf{U}_\mathrm{b} \tag{10}$$

where $\boldsymbol{G}_\mathrm{b}$ is the branch admittance matrix of $(b \times b)$. Substitute (6) (8) into (7), we can get

$$\mathbf{I}_n = -\mathbf{B}^T\mathbf{G}_\mathrm{b}\mathbf{B}\mathbf{U}_\mathrm{n} \tag{11}$$

Supposing that $\boldsymbol{U}_\mathrm{n}$ is determined, according to (11), the distribution of $\boldsymbol{I}_\mathrm{n}$ only relates to the structure of grid. When one or more transformers are operated in parallel in a substation, as a result all neutral point of the transformers will be grounded simultaneously, so the current flowing through this substation will be equally distributed across all the transformers, which means it can reduce the bias risk for each transformer but bring higher cost in protection. In addition, if the earth resistivity is defined, the electric potential in each neutral point will present a trend in linear increase or decrease with the distance change as shown in Fig. 7. Therefore, in general we can say the closer the substation is to the HVDC grounding electrode, the higher the electric potential will have, and the potential difference in neutral points will be obvious when it is connected to another relative far transformer systems, so the DC in this loop will be more serious.

However, to make the situation mentioned above happen, the two substations' distances to grounding electrode shall be significantly different. Otherwise, there will be no significant potential difference between the two and there will be no large current in the loop.

Based on the analysis above, we propose the implementation strategy as follows:

Step 1: According to the DC limits of 12 A and 8 A, give priority to the substations that are in most serious bias risk and more branches to manage.

Step 2: Based on the results in step 1, give priority protection to the substations that having least parallel transformers to reduce the protection cost.

Step 3: After installing resistor devices, observe whether the neutral point DC of the station is within the threshold. If yes, calculate whether the equivalent bias current is lower than 4 A. If the current limit is reached, the subsequent treatment is performed; otherwise, replace the resistor with a capacitor for calculation and analysis. If the bias current of the station still cannot be suppressed, keep the station connected to the device, and select the substation(s) has(have) directly connection to install the suppression device.

Step 4: In order to miss no protection, every protection choice for the substation needs to follow the order mentioned above, till all substations in bias risk are in protection.

IV. VERIFICATION OF THE PROTECTION METHODS

Combined literature [23], We established an AC power grid model as the test subject. The model is based on the actual AC system of Gansu Province, China, which is connected to the Jiuquan-Hunan ±800 kV UHVDC lines. The system includes 15 important substations and the connection frame is shown in Fig. 8.

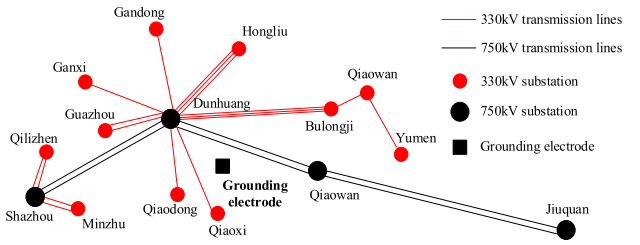

FIGURE 8. Gansu AC system connected to Jiuquan-Hunan UHVDC.

In the model, the DC resistance of the transmission line is equivalent, the multi-circuit line is processed according to the parallel relationship, and the three-winding autotransformer is replaced by the winding DC resistance. Since there is no direct electrical connection between the low voltage winding and the high voltage and medium voltage windings, no direct current is passed, and it is ignored when equivalent. Considering the nature of the loess in Gansu, when the soil model is established, the resistivity correction is performed on the basis of the classical earth model, and the potential distribution of each substation is obtained by numerical calculation. Bring the obtained values into the grid model to calculate the current distribution [24]–[26]. Table 2 shows the soil distribution parameters used.

To verify the model, field measurements were carried out in the actual system. We used DC bias monitoring instrument to detect the current in neutral points. The current direction flowing from transformer to the earth was defined as '+', and the wiring diagram is shown in Fig. 9(a) and Fig. 9(b). Due to experimental setting limits, we were only able to verify the effectiveness of the model with 1500 A ground current.

TABLE 2. Soil resistivity distribution parameters.

Layer	Resistivity (Ω·m)	Thickness (m)
1	60	0~200
2	150	200~2800
3	700	2800~18000
4	13.5	>18000

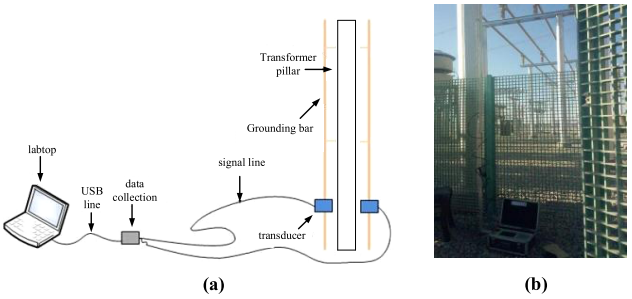

FIGURE 9. DC bias data measurement.

TABLE 3. Comparison between simulation and actual measurement.

substation	Voltage (kV)	1500A measurement (A)	1500A simulation (A)	5000A simulation (A)
Shazhou	750	-30.5	-34.8	-107.7
Qilizhen	330	9.8	11.6	33.4
Minzhu	330	10.3	10.9	35.1
Dunhuang	750	-37.2	-40.4	-130.8
Guazhou	330	31.4	29.8	82.1
Yumen	330	-14.7	-18.3	51.5
Bulongji	330	-2.4	-1.4	-9.3
Hongliu	330	13.1	13.2	45.3
Ganxi	330	1.6	2.1	5.5
Gandong	330	1.2	1.4	4.5
Qiaowan#1	750	-2.2	-2.4	-10.4
Qiaowan#2	330	1.5	2.2	4.8
Jiuquan	750	-0.5	-0.7	-3.9
Qiaodong	330	-16.1	-13.7	59.3
Qiaoxi	330	-46.1	-50.7	-125.2.

Then using the model by numerical simulation, we calculated the most severe situation, namely 5000 A ground current when the system operating at full power. In this case, when there is 5000 A DC flows into the grounding electrode, more than 60% of the substations' transformers have current exceed the limit. The simulation and measured data pairs are shown in Table 3.

It can be seen from Table 3 that the simulation results show the same change law and trend as the field measured data, and the error rate is basically below 10%. The average error rate of simulation results and measured values of Blongji,

TABLE 4. DC current distribution in AC system(part).

substation	Voltage (kV)	capacitor	resistor	I_0 (A)	I_{eff} (A)
Shazhou	750	√		0	-2.1
Qilizhen	330		√	1.2	1.1
Minzhu	330		√	0.9	0.4
Dunhuang	750	√		0	-3.2
Guazhou	330	√		0	-0.8
Yumen	330		√	-2.3	-1.5
Bulongji	330			-4.5	-0.6
Hongliu	330		√	1.3	1.6
Ganxi	330			2.1	0.5
Gandong	300			2.2	0.6
Qiaowan#1	750			-3.8	-0.2
Qiaowan#2	330			0.7	0.3
Jiuquan	750			-0.1	-0.1
Qiaodong	330		√	2.4	0.2
Qiaoxi	330	√		0	-0.1

Ganxi, Gandong and Jiuquan, which are farther away from the grounding electrode, is relatively large. The reason for the error is that the base of the neutral point measurement current of these power stations is itself small, and these currents are within the governance threshold and do not exceed the load carrying capacity of the transformer. Therefore, these power stations are not the main protection targets of DC bias, and will not cause misjudgment during governance.

Based on the protection strategy proposed in this paper, it is determined that 9 substations shall be protected with setup shown in Table 4, where 5 substations use resistors devices and 4 use capacitor devices. Further calculation of equivalent bias current I_{eff} shows that the DCs in all transformers are in good control.

According to Table 4, after taking corresponding measures for each substation, the global DC bias current of the power grid is reduced from 708.8 A to 21.3 A, and the suppression rate is over 90%. It can also be seen that the DC current in the winding is also suppressed to an acceptable range when observing the equivalent bias current I_{eff}. Compared with the single-capacitor resistance straightening method, after a reasonable protection configuration strategy, this method effectively improves the resource utilization based on the DC offset protection effect.

V. CONCLUSION

This paper propose a feasible RC combined method along with an implementation strategy to protect the AC system of Jiuquan-Hunan ±800 kV UHVDC transmission lines from DC bias. With the proposed strategy of 4 steps, a protection scheme was obtained for the 15 substation AC system connected to the UHVDC lines. Numerical simulation of the system operating in full power shows that the proposed method is effective in DC bias control for this DC-AC system operating with the highest voltage up to now.

REFERENCES

[1] D. Chen, Z. Feng, Q. Wang, L. Fang, and B. Bai, "Study of analysis and experiment for ability to withstand DC bias in power transformers," *IEEE Trans. Magn.*, vol. 54, no. 11, Nov. 2018, Art. no. 8401406.
[2] B. Zhao, Q. Song, W. Liu, and Y. Zhao, "Transient DC bias and current impact effects of high-frequency-isolated bidirectional DC–DC converter in practice," *IEEE Trans. Power Electron.*, vol. 31, no. 4, pp. 3203–3216, Apr. 2016.
[3] L. Mingjie, "Characteristic analysis and operational control of large-scale hybrid UHV AC/DC power grids," *Power Syst. Technol.*, vol. 40, no. 4, pp. 985–991, 2016.
[4] B. Tang, X. Zhang, G. Ge, J. G. Zhang, X. F. Liu, and Z. Qu, "Interference on geoelectric field observation from UHVDC power lines and its ground electrode," *High Voltage Eng.*, vol. 39, no. 12, pp. 2951–2959, 2013.
[5] Z. Xie *et al.*, "Advanced DC bias suppression strategy based on finite DC blocking devices," *IEEE Trans. Power Del.*, vol. 32, no. 6, pp. 2500–2509, Dec. 2017.
[6] Z. Pan *et al.*, "Potential compensation method for restraining the DC bias of transformers during HVDC monopolar operation," *IEEE Trans. Power Del.*, vol. 31, no. 1, pp. 103–111, Feb. 2016.
[7] Z. Wang *et al.*, "Novel DC bias suppression device based on adjustable parallel resistances," *IEEE Trans. Power Del.*, vol. 33, no. 4, pp. 1787–1797, Aug. 2018.
[8] S. N. Vukosavic and L. S. Perić, "High-precision active suppression of DC bias in AC grids by grid-connected power converters," *IEEE Trans. Ind. Electron.*, vol. 64, no. 1, pp. 857–865, Jan. 2017.
[9] X. Zhao, J. Lu, L. Li, Z. Cheng, and T. Lu, "Analysis of the DC bias phenomenon by the harmonic balance finite-element method," *IEEE Trans. Power Del.*, vol. 26, no. 1, pp. 475–485, Jan. 2011.
[10] Z. Chen, B. Bai, D. Chen, and W. Chai, "Direct-current and alternate-decay-current hybrid integrative power supplies design applied to DC bias treatment," *IEEE Trans. Power Electron.*, vol. 33, no. 12, pp. 10251–10264, Dec. 2018.
[11] Q. Wang, R. Gong, J. Ruan, Y. Wu, C. Liu, and S. Jin, "The calculation and suppression of the AC Grid DC bias current under the monopole operation of UHVDC system," in *Proc. IEEE Int. Conf. High Voltage Eng. Appl.*, Sep. 2016, pp. 1–4.
[12] X. Wen, T. Guo, Z. He, Q. Yang, and H. Lu, "Review on the related problems of DC magnetic bias," *High Voltage App.*, vol. 52, no. 6, pp. 1–8, 2016.
[13] Z. Yanli, W. Jiayin, and B. Baodong, "Influence analysis of DC biased magnetic field on magnetostrictive characteristics of silicon steel," *Proc. CSEE*, vol. 36, no. 15, pp. 4299–4306, 2016.
[14] C. Zhiwei, B. Baodong, and C. Dezhi, "Research on the formation mechanism and supperssion method of transformer DC bias," *Trans. China Electrotechnical Soc.*, vol. 30, no. 14, pp. 208–214, 2015.
[15] M. Mu, F. Zheng, Q. Li, and F. C. Lee, "Finite element analysis of inductor core loss under DC bias conditions," *IEEE Trans. Power Electron.*, vol. 28, no. 9, pp. 4414–4421, Sep. 2013.
[16] Z. Tao, Z. Xianqi, H. Dongwei, and L. Lianguang, "Influence of grid-connected DC suppression device on distance protection of transmission line," *Power Syst. Technol.*, vol. 37, no. 2, pp. 545–550, 2013.
[17] C. Han, L. Wang, Z. Zhang, J. Xie, and Z. Xing, "A multi-objective genetic algorithm based on fitting and interpolation," *IEEE Access*, vol. 6, pp. 22920–22929, 2018.
[18] L.-X. Wei, X. Li, R. Fan, H. Sun, and Z.-Y. Hu, "A hybrid multiobjective particle swarm optimization algorithm based on R2 indicator," *IEEE Access*, vol. 6, pp. 14710–14721, 2018.
[19] C. Nan, W. Tianzheng, and W. Dongqing, "Study on configuration optimization method of transformer magnetic bias treatment," *Power Syst. Protection Control*, vol. 45, no. 10, pp. 117–122, 2017.
[20] X. Zhicheng, L. Xiangning, and L. Zhengtian, "Suppression method for DC bias based on global optimal witching method of blocking devices," *Proc. CSEE*, vol. 37, no. 24, pp. 7133–7142, 2017.
[21] H. Takshi, G. Dogan, and H. Arslan, "Joint optimization of device to device resource and power allocation based on genetic algorithm," *IEEE Access*, vol. 6, pp. 21173–21183, 2018.
[22] J.-F. Qiao, C. Lu, and W.-J. Li, "Design of dynamic modular neural network based on adaptive particle swarm optimization algorithm," *IEEE Access*, vol. 6, pp. 10850–10857, 2018.

[23] H. Caichen, "Research on the optimal configuration of suppressing transformer DC bias magnetic capacitance blocking device," M.S. thesis, North China Electr. Power Univ., Beijing, China, 2016.
[24] D. S. Gazzana, A. B. Tronchoni, R. C. Leborgne, A. S. Bretas, D. W. P. Thomas, and C. Christopoulos, "An improved soil ionization representation to numerical simulation of impulsive grounding systems," *IEEE Trans. Magn.*, vol. 54, no. 3, Mar. 2018, Art. no. 7200204.
[25] C. M. Seixas and S. Kurokawa, "A grounding system model directly in time-domain," *IEEE Latin Amer. Trans.*, vol. 14, no. 10, pp. 4261–4266, Oct. 2016.
[26] M. Chenglian, L. Lianguang, and W. Letian, "The ANSYS simulation of HVDC grounding electrode potential distribution," *Power Syst. Clean Energy*, vol. 33, no. 4, pp. 19–26, 2017

JIANGONG ZHANG was born in Hubei, China, in 1975. He received the B.S. degree in electrical engineering from the Huazhong University of Science and Technology, Wuhan, China, in 2006. He is currently a Senior Engineer with the China Electric Power Research Institute. His research interests include electromagnetic transient process in substation as well as space-charge field computation of HVDC.

BOCHENG LI was born in Gansu, China, in 1996. He received the B.S. degree in power transmission line engineering from the College of Science and Technology, China Three Gorges University, in 2018. He is currently pursuing the M.S. degree with China Three Gorges University. His research interest includes power transmission line engineering.

BO TANG was born in Hubei, China, in 1978. He received the Ph.D. degree in electrical and electronic engineering from the Huazhong University of Science and Technology, in 2011. He is currently an Associate Professor with China Three Gorges University. His research interests include power transmission line engineering and electromagnetic environment of power systems.

JIAWEI YANG was born in Gansu, China, in 1994. He received the B.S. degree in power transmission line engineering from the College of Science and Technology, China Three Gorges University, in 2016. He is currently pursuing the M.S. degree with China Three Gorges University. His research interest includes power transmission line engineering.

LI HUANG was born in Hubei, China, in 1980. He received the Ph.D. degree in electrical and electronic engineering from Uiduk University, in 2016. He is currently with China Three Gorges University. His research interests include high voltage technology, applied superconductivity, and electromagnetic analysis.